

LAGRANGIAN VERSUS EULERIAN METHODS FOR TOROIDALLY-MAGNETIZED ISOTHERMAL DISKS

YASHVARDHAN TOMAR¹ AND PHILIP F. HOPKINS^{1*}

¹TAPIR, Mailcode 350-17, California Institute of Technology, Pasadena, CA 91125, USA
Version December 8, 2025

ABSTRACT

A number of simulations have seen the emergence of strongly-toroidally-magnetized accretion disks from interstellar medium inflows. Recently, Guo et al. (2025) (G25) studied an idealized test problem of toroidally-magnetized disks in isothermal ideal MHD with an Eulerian static-mesh method, and argued the midplane behavior changes qualitatively (with a significant loss of toroidal magnetic flux) when the thermal scale-length is resolved ($\Delta x < H_{\text{thermal}}$). We rerun the G25 test problem with two Lagrangian methods: meshless finite-mass, and meshless finite-volume. We show that Lagrangian methods reproduce the high-resolution ($\Delta x \ll H_{\text{thermal}}$) Eulerian G25 results. At low resolution ($\Delta x \gg H_{\text{thermal}}$), behaviors differ: Lagrangian methods still lose flux and evolve “as close as possible” to the converged solution, while Eulerian methods show no evolution. We argue this difference in convergence behavior is related to the ability of Lagrangian codes to follow flows to an arbitrarily thin midplane layer, analogous to the well-studied difference in Jeans fragmentation problems. This and results from other higher-resolution simulations and different codes suggest that the sustained midplane toroidal fields seen in recent Lagrangian multi-scale, multi-physics simulations cannot be a numerical resolution effect, and some physical difference between those simulations and the G25 test problem explains their different behaviors.

Subject headings: methods: numerical — hydrodynamics — galaxies: formation — cosmology: theory

1. INTRODUCTION

A number of studies have argued that accretion disks around AGN in particular could be strongly magnetized, with primarily toroidal magnetic fields and midplane magnetic $\beta_{\text{th}} \equiv P_{\text{gas, thermal}}/P_{\text{B}} \ll 1$ (Gaburov et al. 2012; Guo et al. 2024; Shi et al. 2024b; Hopkins et al. 2024b,a,c, 2025; Kaaz et al. 2025; Wang et al. 2025). In all of these simulations, the disks emerge from attempts to more self-consistently model the accretion process from large-to-small scales with inflows from interstellar medium-type scales and structures. This is essential to understand, as it could radically change our understanding of the accretion disk structure, support for phases like the broad-line region and Comptonizing layers, line-driven winds, and many other properties and puzzles of AGN observations (references above and Hopkins 2025).

In order to better understand these disks, Squire et al. (2025) (S25) and Guo et al. (2025) (G25) performed some idealized experiments, both using static Cartesian grids in ATHENA, with isothermal, ideal MHD in an analytic Keplerian potential and no other physics. S25 considered a shearing-box, with different initial toroidal field strengths, while G25 considered the collapse of a homogeneous, uniformly rotating and uniformly magnetized sphere. Both found that when their spatial resolution was too poor – specifically when $\Delta x \gtrsim H_{\text{thermal}} = c_s/\Omega$ in terms of the thermal scale-length H_{thermal} , isothermal sound speed c_s and Keplerian $\Omega = \sqrt{GM}/r^3 = v_K/r$ – the initial magnetization of the midplane was maintained indefinitely, however it was set. But when G25 increased their resolution to $\Delta x < H_{\text{thermal}}$, they eventually (after hundreds of dynamical times) saw a “vertical collapse” of the midplane to a dense, sharply-peaked layer with midplane $\beta \sim 1$ (though a very thick layer with $\beta \ll 1$, containing an order-unity fraction of the total mass and much of the total accretion rate through the disk, still persisted indefinitely at all resolution levels). S25 showed consistent results, and how this related to the shutdown of a quasi Parker dynamo (as originally hypothesized in Johansen

& Levin 2008).

However the static, Cartesian meshes used for these tests are numerically quite different from many of the original motivating simulations which use Lagrangian or quasi-Lagrangian numerical methods. And it is known that various collapse test problems often exhibit qualitatively different behavior between Eulerian and Lagrangian methods (see § 3). We therefore repeat the experiment in G25 using multiple Lagrangian methods, to inform our interpretation of toroidally-magnetized disks and numerical convergence criteria for their behavior. § 2 describes the problem setup and tests. § 3 discusses how this relates to other known differences between Lagrangian and Eulerian methods, and § 4 discusses the implications for the multi-physics simulations above. We summarize in § 5.

2. METHODS & TESTS

We initialize the test problem from G25, to which we refer for details. Briefly, we evolve the equations of ideal MHD without self-gravity in an analytic Keplerian potential with $G = M = 1$, with an inner outflow/sink boundary at $r_0 = 1$ and initial uniform gas density $\rho_0 = 1$, velocity $\mathbf{v}_0 = v_{\phi,0}\hat{\phi}$, $v_{\phi,0} = \sqrt{GMR_{\text{circ}}}/R$ with $R_{\text{circ}} = 16r_0$ and R the cylindrical radius, and $\mathbf{B}_0 = B_{\phi,0}\hat{\phi}$, $B_{\phi,0} = 0.0045$, outside of an initial “tapering” region (at $R < 8R_0$) defined in G25. The equation-of-state is set to be strictly locally-isothermal with $h \equiv c_s/v_K = c_s\sqrt{R/GM} = 0.05$, with a minimum $c_{s,\text{min}} \approx 0.003$. The outer boundary is open but we only initialize gas out to a radius where the free-fall time is long compared to the time to which we evolve the simulations, so it has no effect. We implement this in the code GIZMO (Hopkins 2015),¹ using the second-order reconstruction and HLLD solver. GIZMO is a multi-method code and we consider several different numerical methods: our default setup uses the meshless finite-mass (MFM) method for consistency with Hopkins et al. (2024b), but we also consider

*E-mail: phopkins@caltech.edu

¹ A public version of the code (Hopkins 2017) is available at <http://www.tapir.caltech.edu/~phopkins/Site/GIZMO.html>.

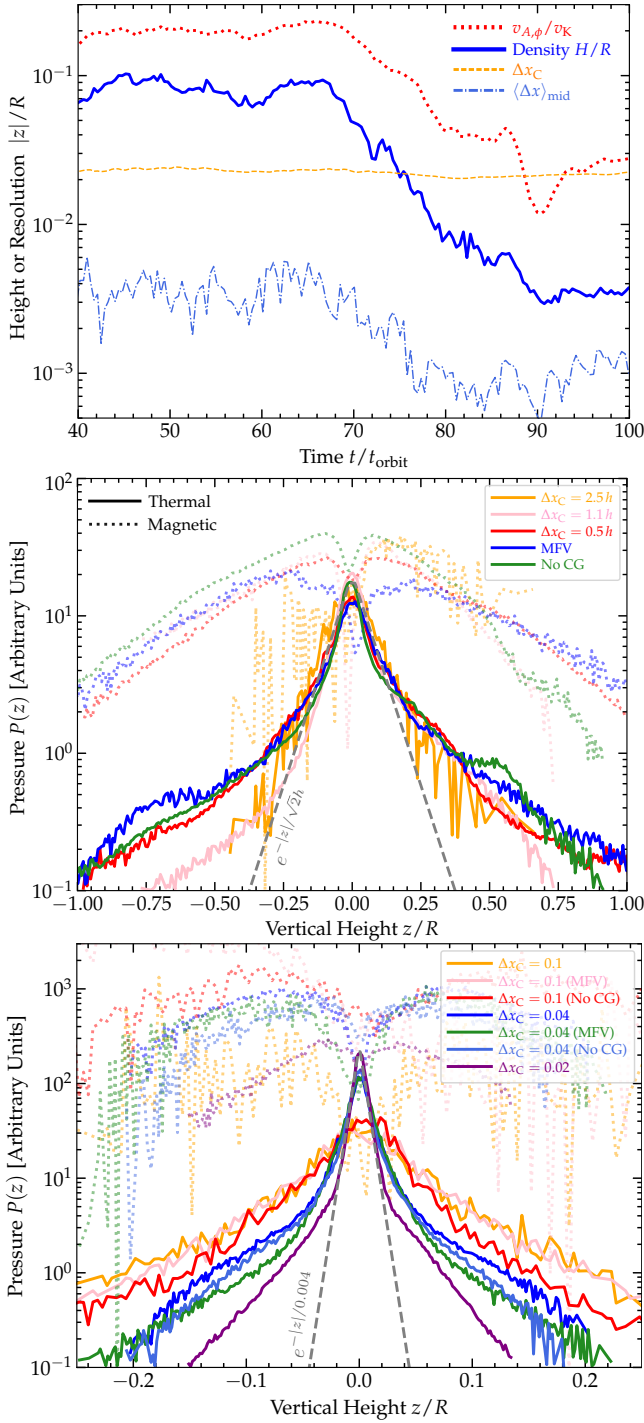


FIG. 1.— G25 collapsing disk test problem (§ 2). *Top:* Time evolution in an example with *unresolved* thermal scale-height owing to extremely low- β ($h = 10^{-4}$), with Lagrangian MFM. Around the circularization radius, we plot the Alfvén scale-height $v_{A,\phi}/v_K$ and midplane density scale-height H/R in cylinders, with the Cartesian-equivalent resolution $\Delta x^C = (\text{Volume}/N_{\text{cells}})^{1/3}$ and median Lagrangian resolution near the midplane $\langle \Delta x \rangle^{\text{mid}}$ (both in units of R), at times after the initial disk forms until “collapse” as defined by G25 occurs. *Middle:* Vertical thermal ($P_{\text{th}} = \rho c_s^2 \propto \rho h^2$) and magnetic ($P_B = B_\phi^2/2$) pressure profiles at the scale-height minimum of Lagrangian simulations with $h = 0.05$. We show MFM at three resolution levels, plus an MFV run and a run without constrained-gradient MHD. We compare an exponential profile $\rho \propto \exp(-|z|/\sqrt{2}h)$. Converged solutions collapse to midplane $\beta \sim 1$ and scale-height $\sim \sqrt{2}h$. *Bottom:* Same, for runs with $h = 10^{-4}$. The behavior seen is similar to the “high-resolution” ($\Delta x^C < h$) tests in G25, where H/R decreases after tens of orbits, $\rho(z)$ forms a steep peak, and P_B features a decrement around $|z| \sim 0$. With Lagrangian methods, collapse begins even with $\Delta x^C \gg h$, until the disk is ~ 1 -cell thick.

meshless finite-volume (MFV) and (low-resolution-only) fixed Cartesian-mesh simulations. We also consider MFM with both the constrained-gradient CG-MHD (Hopkins 2016) reconstruction method as used in Hopkins et al. (2024b), or without this as in Hopkins & Raives (2016). We analyze the gas around R_{circ} , as G25: defining “collapse” by the evolution of H_ρ/R , the density scale-height (defined as the median mass-weighted $|z|$ in a narrow annulus around R_{circ}) and H_B/R , the Alfvén scale-height defined by $H_B \equiv v_{A,\phi}/\Omega = |B_\phi|/\sqrt{\rho}\Omega$ where B_ϕ is measured in a small cylindrical ring with vertical extent $-H_\rho/2 < z < H_\rho/2$. The thermal scale-height $H_{\text{thermal}}/R = c_s/v_K \equiv h = 0.05$, by construction. We also consider a test where H_{thermal} is set much smaller (intentionally unresolvable), multiplying c_s and therefore h uniformly by 0.002 (so $h = 10^{-4}$).

The effective resolution $\Delta x/R$, at the same radii, is not trivial to estimate in these numerical methods. We therefore consider three definitions. First, an “equivalent Cartesian” spatial resolution $\langle \Delta x \rangle^C \equiv (\text{Volume}/N)^{1/3}$, counting the total number of particles and volume in a cylindrical annulus $R - \Delta R/2 < R < R + \Delta R/2$ with $\Delta R = R/2$ and $|z| < R$. Second, the median actual resolution in the midplane region $\langle x \rangle^{\text{mid}}$, defined by the median $\Delta x \equiv (\Delta m/\rho)^{1/3}$ of all cells within the small cylindrical ring around the midplane with $-H_\rho/2 < z < H_\rho/2$. Third, the resolution at which vertical structure in the Lagrangian code would become ill-defined, i.e. the disk would be effectively “one cell thick,” defined as in Hopkins et al. (2024b) by the cell separation which would be present if all cells within an annulus were placed in the midplane, $\langle \Delta x \rangle^{2d} \equiv (\text{Area}/N)^{1/2}$ in terms of the annular area and N used for $\langle \Delta x \rangle^C$.

Fig. 1 shows the numerical results from these tests. Although for Eulerian methods with poor resolution $\Delta x \gtrsim H_{\text{thermal}}$, the disk thickness and B_ϕ are maintained, in all of our Lagrangian tests, we see the a similar “collapse” begin as seen only at high resolution in Eulerian methods. Specifically, we see a decrease in time of the midplane density scale-height as a steep density “spike” forms at $|z| \sim h$, with a thicker, $\beta \ll 1$ envelope which contains an $O(1)$ fraction of the total disk mass, and a “dimple” or decrease in the central magnetic pressure. The converged ($h = 0.05$) Eulerian and Lagrangian solutions agree that collapse proceeds until $\beta \sim 1$ (density scale-height $\sim h$) in the midplane. However the low-resolution behavior differs: in Eulerian tests in S25 & G25, no collapse or flux loss appears if $\langle \Delta x \rangle^C \gtrsim H_{\text{thermal}}$. In Lagrangian methods, the “beginning” of collapse appears to be essentially resolution-independent, even for $\langle \Delta x \rangle^C \gg H_{\text{thermal}}$. This is most obvious in the runs with extremely low- β ($h = 10^{-4}$). As we approach the cold plasma limit ($\beta \rightarrow 0$, $h \rightarrow 0$), the Lagrangian methods cannot resolve the $\beta \sim 1$ scale height h , so the code simply collapses to its effective resolution limit, $\sim \langle \Delta x \rangle^{2d}$, and so gets denser as we increase the resolution (approaching the converged solution). We see broadly similar results for MFM and MFV and runs with/without CG-MHD.

There are some subtleties that may differ from G25 in the converged solutions: we see (as they noted) a strong association between overdense rings/spiral structures and vertical collapse, but the causal relationship is unclear. Still as these move “through” a given annulus the degree of collapse can vary, and sometimes warps excited by grid noise from the collapsing material can “stir up” some regions. But these do not change our conclusions.

3. INTERPRETATION AND RELATION TO OTHER LAGRANGIAN-EULERIAN DIFFERENCES

There are some potentially simple interpretations of the difference at low resolution between Eulerian and Lagrangian methods in the G25 problem. In Eulerian fixed-mesh codes, Δx at the midplane is fixed, and it is impossible to represent vertical structure/gradients in any field (ρ , \mathbf{B} , \mathbf{v}) below some multiple of Δx . Per S25/G25, when Δx is too large, this makes it impossible for the Parker dynamo as described in [Johansen & Levin \(2008\)](#); [Gaburov et al. \(2012\)](#) and S25 to shut itself off, and therefore prevents Parker modes from removing magnetic flux from scales $|z| \lesssim \Delta x$. In Lagrangian codes, there are two important qualitative differences. First, for a nominal Cartesian-equivalent $\langle \Delta x \rangle^C$, the *actual* vertical resolution $\langle \Delta x \rangle^{\text{mid}}$ of the simulation around the midplane can be vastly superior, as by definition more gas will be concentrated towards the midplane, and any effect which attempts to initiate an increase in the midplane density (e.g. the early states of collapse) will lead to even better spatial resolution in the midplane. Indeed this one of the major motivations for Lagrangian methods in disk problems, in the first place. Second, in Lagrangian methods, cells *move*, so it is always possible in principle for modes to carry magnetic flux away from the midplane with said cells, even in the limit when all cells have piled up in the midplane such that vertical gradients become numerically ill-defined ($\langle \Delta x \rangle^{\text{mid}} \rightarrow \langle \Delta x \rangle^{2d}$). This explains why even taking $h \rightarrow 0$, we still see collapse (just down to the single-cell resolution limit, rather than h).

This is analogous to other, better-studied differences between Eulerian and Lagrangian codes on collapse problems, perhaps most notably the “artificial fragmentation” problem. In simple test problems of seeded Jeans fragmentation in a homogeneous self-gravitating medium, as well as more complex problems, it is well-established (see e.g. [Truelove et al. 1997, 1998](#); [Banerjee et al. 2004](#)) that in Eulerian (static or adaptive mesh refinement) methods, if $\Delta x > \lambda_J \equiv c_s / \sqrt{G\rho}$, numerically spurious modes begin to grow, and the mass/size distribution of fragments can be corrupted (causing “over-fragmentation”) on scales much larger than Δx . But it is equally well-established that this error does not appear in Lagrangian methods (including SPH, MFM, and MFV; [Hubber et al. 2006](#); [Chiaki & Yoshida 2015](#); [Manuel et al. 2016](#); [Guszejnov et al. 2018](#); [Yamamoto et al. 2021](#)). So long as one uses a (required and always true in modern codes like GIZMO) consistent definition of force softening and hydrodynamic resolution, then in Lagrangian codes there is no over-fragmentation: instead the error if the Jeans length is unresolved ($\Delta x > \lambda_J$, equivalent to saying the Jeans mass is unresolved $\Delta m > M_J$) is simply the obvious one that collapse of fragments approaching the resolution limit (near single-cell) is slowed down, and obviously no fragments can form below the resolution Δm . Similar results hold for magnetized Jeans collapse ([Myers et al. 2013](#); [Guszejnov et al. 2020](#)) and disk fragmentation ([Robertson & Kravtsov 2008](#); [Deng et al. 2017](#); [Forgan et al. 2017](#); [Deng et al. 2021](#); [Xu et al. 2025a,b](#)). The generally-accepted interpretation of this is similar to our argument above: in Lagrangian codes, the fact that the cell size and mesh-generating point positions are shrinking and moving continuously with the fluid in the compressive modes means that the salient numerical error terms cannot propagate to larger scales.

On top of these, in different codes, the thermal speed can play a non-trivial role in numerical dissipation/viscosity, even in problems approaching the cold plasma limit. In cold shear-

ing disks studies ([Imaeda & Inutsuka 2002](#); [Hopkins 2015](#); [Schaal et al. 2015](#); [Duffell 2016](#); [Zier & Springel 2022](#), and references therein), it is known that static Cartesian mesh methods like those used in G25 suffer from certain numerical errors and instabilities which are suppressed when the thermal scale-height is well-resolved. If these effects are important, we would expect a difference in this problem in Eulerian codes using Cartesian vs. well-aligned curvilinear meshes, or shearing boxes, so the similarity of S25 and G25 suggests this may not be a dominant effect.

4. DISCUSSION: IMPLICATIONS FOR OTHER TOROIDALLY-MAGNETIZED DISK SIMULATIONS

Strongly toroidally-magnetized disks have now been seen with a number of different codes using different numerical methods, including: FVMHD3D ([Gaburov et al. 2012](#)), a Voronoi-tessellation based moving-mesh finite-volume scheme, in simulations of molecular cloud collisions with a black hole ([Gaburov et al. 2012](#)); ATHENA-K ([Stone et al. 2024](#)), with Eulerian static-but-nested Cartesian meshes, in ideal-MHD plus cooling simulations of low-level Bondi accretion of hot gas from galaxy to supermassive black holes ([Guo et al. 2024](#)); ATHENA-K with similar nested meshes in ideal-MHD plus cooling simulations of collapse of turbulent clouds onto binary supermassive black holes ([Wang et al. 2025](#)); GIZMO ([Hopkins 2016](#)), with Lagrangian meshless-finite-mass (MFM) and meshless-finite-volume (MFV) methods, in simulations of high-redshift starburst galactic flows to supermassive black holes as quasars ([Hopkins et al. 2024b,a,c, 2025](#)); GIZMO using the MFM solver but a different numerical MHD method ([Hopkins & Raives 2016](#)), in simulations of molecular-cloud and star-cluster accretion onto intermediate-mass black holes ([Shi et al. 2024b,a](#)); ENZO ([O’Shea et al. 2004](#)), with Eulerian Cartesian adaptive mesh refinement (AMR), in ideal-MHD simulations of gas inflows around first-stars ([Luo & Shlosman 2024](#)); and H-AMR ([Liska et al. 2022](#)), a general-relativistic MHD code using a static-mesh-refinement (SMR) spherical coordinate grid, in simulations ([Kaaz et al. 2025](#)) of inflows to horizon scales using an initial condition from [Hopkins et al. \(2024b\)](#).

This raises important questions. Could this imply that the persistence of toroidally-magnetized disks in the simulations owes to lack of resolution? This seems unlikely, as the simulations in [Shi et al. \(2024b,a\)](#); [Hopkins et al. \(2024b, 2025\)](#) had $\Delta x \sim 0.01 - 0.1 H_{\text{thermal}}$ for the diffuse, volume-filling midplane gas, although their disks were multi-phase so they contain cold gas clouds with much smaller H_{thermal} . The highest-resolution run in [Gaburov et al. \(2012\)](#), which was isothermal, had $\Delta x \approx 0.33 H_{\text{thermal}}$. [Hopkins et al. \(2025\)](#) re-ran multiple versions of their disks enforcing a temperature floor such that $\Delta x \lesssim 0.1 H_{\text{thermal}}$ for all gas. [Kaaz et al. \(2025\)](#) ran for extended durations with an simplified effective equation of state (for radiation+gas) such that there was a well-defined $\Delta x \sim 0.02 - 0.05 H_{\text{thermal}}$ in the toroidally-magnetized zone. And [Luo & Shlosman \(2024\)](#) had $\Delta x \sim 0.03 H_{\text{thermal}}$ in their outer disk, though these disks also had strong poloidal fields. All of these meet the G25 “high-resolution” criterion. Moreover, our tests indicate that the Lagrangian simulations, including those from GIZMO and FVMHD3D (and perhaps ENZO, which is quasi-Lagrangian with AMR and so might exhibit some Lagrangian characteristics, but this is not obvious), can reproduce the initial vertical collapse and toroidal flux loss of G25 even at much worse resolution (they would just collapse to ~ 1 cell thick, which clearly does not hap-

pen in those simulations). Plus, all these simulations contain some non-negligible (if not dominant) poloidal field, which G25 found aided in maintaining midplane $\beta \ll 1$ at high resolution. So this very clearly argues that the sustained toroidal fields in those simulations are not a numerical artifact.

Alternatively, could this imply that the “collapse” seen in S25 and G25 is a numerical artifact? Those simulations used static, Cartesian, Eulerian grids, which are well-known to be much more numerically diffusive/resistive in thin-disk problems (see e.g. Hahn et al. 2010; Duffell & MacFadyen 2011, 2012; Duffell et al. 2024; Mocz et al. 2014; Muñoz et al. 2014; Hopkins 2015; Seo et al. 2019; Deng et al. 2019, 2020b,a; Deng & Ogilvie 2022) compared to either Eulerian spherical/cylindrical coordinate grids (like in Kaaz et al. 2025) or Lagrangian grids (like in Gaburov et al. 2012; Hopkins et al. 2024b; Shi et al. 2024b). S25, for example, saw the midplane β increase from an initially low value to $\beta \sim 1$ as their resolution improved from $\Delta x \approx H_{\text{thermal}}$ to $\Delta x \approx 0.4 H_{\text{thermal}}$, but then saw the midplane β gradually decrease again steadily with further resolution improvements up to their highest resolution $\Delta x \approx 0.07 H_{\text{thermal}}$, without an obvious indication of convergence. But our results imply that collapse on this test problem is not purely an artifact of the Eulerian method, since we see the same collapse in Lagrangian simulations with different methods, although we cannot definitively answer the question of convergence in this test problem either (as we do not replicate S25).

Instead, our results argue that the difference between the idealized, symmetric, non-turbulent, strictly isothermal ideal-MHD simulation tests in S25, G25, and herein, and the multi-scale, multi-physics simulations above, likely owes to some real physics or initial/boundary conditions. There is no shortage of plausible candidates, as discussed in e.g. Hopkins et al. (2024b): the simulations in Hopkins et al. (2024b,a,c, 2025); Kaaz et al. (2025); Luo & Shlosman (2024); Shi et al. (2024b,a); Wang et al. (2025) not only include much more complex, multi-phase, turbulent, highly dynamic, inhomogeneous, non-spherical boundary/initial conditions, but they also include physics like self-gravity, multi-group radiation-hydrodynamics and radiation pressure, multi-phase gas thermo-chemistry with complex equations-of-state, general relativity, star formation and stellar feedback, collisionless (stars+dark matter) plus gas components, highly asymmetric disks with strong global modes and spiral arms, etc. So the challenge is isolating any single piece of physics that could be most important. A hint might come from the more simplified ideal-MHD, analytic-gravity simulations in Gaburov et al. (2012) which also adopted a simple locally-isothermal equation-of-state, but whose initial condition allowed for a

more turbulent and asymmetric (eccentric with strong global modes) disk, with a much larger accretion/inflow (and therefore toroidal flux *replenishment*) rate than G25. Alternatively the simulations in Wang et al. (2025) adopt a turbulent initial condition, with simplified but multi-phase gas cooling, and an asymmetric time-dependent (binary) analytic background. And as noted above all these more complex simulations included non-trivial poloidal field structure as well.

5. SUMMARY

We reproduce the test problem from G25 – collapse of a homogeneous, uniformly rotating and magnetized sphere in isothermal ideal-MHD with Keplerian gravity – with multiple Lagrangian methods. We show that Lagrangian methods reproduce the high-resolution behavior of the G25 Eulerian tests, wherein the midplane becomes denser with $\beta \sim 1$. S25 and G25 showed that in Eulerian codes, seeing almost any flux loss or density increase requires resolving the thermal scale-length of the disk, $\Delta x < H_{\text{therm}} = c_s/\Omega$. But in Lagrangian methods, the initial flux loss and density increase is recovered at all resolution levels even when the thermal scale-length is arbitrarily poorly-resolved. In the unresolved limit, collapse simply proceeds until the midplane reaches single-cell thickness (reaching “as close as possible” to the high-resolution solution). We argue this owes to the fundamentally different behavior of Lagrangian methods in their ability to follow vertical motions and structure in the limit where the thermal scale-length is unresolved. This is analogous to other well-studied differences between Lagrangian and Eulerian codes, notably their very different behaviors in Jeans fragmentation.

This argues that the *lack* of such collapse – i.e. sustained, strong toroidal fields – seen in the multi-physics simulations which motivated S25 and G25, is numerically robust. In other words, in addition to the fact that the simulations and numerical tests in Hopkins et al. (2024b, 2025); Kaaz et al. (2025); Luo & Shlosman (2024) already satisfy the resolution criterion argued for in G25, the fact that the simulations in Hopkins et al. (2024b, 2025); Shi et al. (2024b,a) use the same Lagrangian methods tested here (at much higher resolution), which reproduce collapse in the G25 test problem even at much worse resolution, argues that the lack of such collapse in their multi-physics simulations is not a resolution artifact. A much more likely hypothesis is that some other physics or boundary/initial conditions explains the difference. Future work is clearly called for to identify those key drivers.

We thank Minghao Guo, Eliot Quataert and Jono Squire for helpful discussions. Support for PFH was provided by a Simons Investigator Grant. Numerical calculations were run on NSF TACC allocation AST21010.

REFERENCES

- Banerjee R., Pudritz R. E., Holmes L., 2004, *MNRAS*, **355**, 248
 Chiaki G., Yoshida N., 2015, *MNRAS*, **451**, 3955
 Deng H., Ogilvie G. I., 2022, *MNRAS*,
 Deng H., Mayer L., Meru F., 2017, *ApJ*, **847**, 43
 Deng H., Mayer L., Latter H., Hopkins P. F., Bai X.-N., 2019, *ApJS*, **241**, 26
 Deng H., Ogilvie G. I., Mayer L., 2020a, arXiv e-prints, p. arXiv:2010.00862
 Deng H., Mayer L., Latter H., 2020b, *ApJ*, **891**, 154
 Deng H., Mayer L., Helled R., 2021, *Nature Astronomy*, **5**, 440
 Duffell P. C., 2016, *ApJS*, **226**, 2
 Duffell P. C., MacFadyen A. I., 2011, *ApJS*, **197**, 15
 Duffell P. C., MacFadyen A. I., 2012, *ApJ*, **755**, 7
 Duffell P. C., et al., 2024, *ApJ*, **970**, 156
 Forgan D., Price D. J., Bonnell I., 2017, *MNRAS*, **466**, 3406
 Gaburov E., Johansen A., Levin Y., 2012, *ApJ*, **758**, 103
 Guo M., Stone J. M., Quataert E., Kim C.-G., 2024, arXiv e-prints, p. arXiv:2405.11711
 Guo M., Quataert E., Squire J., Hopkins P. F., Stone J. M., 2025, arXiv e-prints, p. arXiv:2505.12671
 Guszejnov D., Hopkins P. F., Grudić M. Y., Krumholz M. R., Federrath C., 2018, *MNRAS*, **480**, 182
 Guszejnov D., Grudić M. Y., Hopkins P. F., Offner S. S. R., Faucher-Giguère C.-A., 2020, *MNRAS*, **496**, 5072
 Hahn O., Teyssier R., Carollo C. M., 2010, *MNRAS*, **405**, 274
 Hopkins P. F., 2015, *MNRAS*, **450**, 53
 Hopkins P. F., 2016, *MNRAS*, **462**, 576
 Hopkins P. F., 2017, ArXiv e-prints, arXiv:1712.01294,
 Hopkins P. F., 2025, *The Open Journal of Astrophysics*, **8**, 56
 Hopkins P. F., Raives M. J., 2016, *MNRAS*, **455**, 51

- Hopkins P. F., et al., 2024a, *The Open Journal of Astrophysics*, **7**, 18
- Hopkins P. F., et al., 2024b, *The Open Journal of Astrophysics*, **7**, 19
- Hopkins P. F., Grudic M. Y., Kremer K., Offner S. S. R., Guszejnov D., Rosen A. L., 2024c, *The Open Journal of Astrophysics*, **7**, 71
- Hopkins P. F., et al., 2025, *The Open Journal of Astrophysics*, **8**, 48
- Hubber D. A., Goodwin S. P., Whitworth A. P., 2006, *A&A*, **450**, 881
- Imaeda Y., Inutsuka S.-i., 2002, *ApJ*, **569**, 501
- Johansen A., Levin Y., 2008, *A&A*, **490**, 501
- Kaaz N., Liska M., Tchekhovskoy A., Hopkins P. F., Jacquemin-Ide J., 2025, *ApJ*, **979**, 248
- Liska M. T. P., et al., 2022, *ApJS*, **263**, 26
- Luo Y., Shlosman I., 2024, *ApJ*, **976**, 85
- Manuel Z.-A., Enrique V.-S., Bastian K., Robi B., Lee H., 2016, *MNRAS*, in press, arXiv:1606.05343,
- Mocz P., Vogelsberger M., Sijacki D., Pakmor R., Hernquist L., 2014, *MNRAS*, **437**, 397
- Muñoz D. J., Kratter K., Springel V., Hernquist L., 2014, *MNRAS*, **445**, 3475
- Myers A. T., McKee C. F., Cunningham A. J., Klein R. I., Krumholz M. R., 2013, *ApJ*, **766**, 97
- O’Shea B. W., Bryan G., Bordner J., Norman M. L., Abel T., Harkness R., Kritsuk A., 2004, eprint, arXiv:astro-ph/0403044,
- Robertson B. E., Kravtsov A. V., 2008, *ApJ*, **680**, 1083
- Schaal K., Bauer A., Chandrasekar P., Pakmor R., Klingenberg C., Springel V., 2015, *MNRAS*, **453**, 4278
- Seo W.-Y., Kim W.-T., Kwak S., Hsieh P.-Y., Han C., Hopkins P. F., 2019, *ApJ*, **872**, 5
- Shi Y., Kremer K., Hopkins P. F., 2024a, *A&A*, **691**, A24
- Shi Y., Kremer K., Hopkins P. F., 2024b, *ApJ*, **969**, L31
- Squire J., Quataert E., Hopkins P. F., 2025, *The Open Journal of Astrophysics*, **8**, 39
- Stone J. M., et al., 2024, *arXiv e-prints*, p. arXiv:2409.16053
- Truelove J. K., Klein R. I., McKee C. F., Holliman II J. H., Howell L. H., Greenough J. A., 1997, *ApJ*, **489**, L179+
- Truelove J. K., Klein R. I., McKee C. F., Holliman II J. H., Howell L. H., Greenough J. A., Woods D. T., 1998, *ApJ*, **495**, 821
- Wang H.-Y., Guo M., Most E. R., Hopkins P. F., Lalakos A., 2025, *arXiv e-prints*, p. arXiv:2504.03874
- Xu W., Jiang Y.-F., Kunz M. W., Stone J. M., 2025a, *arXiv e-prints*, p. arXiv:2504.18751
- Xu W., Jiang Y.-F., Kunz M. W., Stone J. M., 2025b, *ApJ*, **986**, 91
- Yamamoto Y., Okamoto T., Saitoh T. R., 2021, *MNRAS*, **504**, 3986
- Zier O., Springel V., 2022, *MNRAS*, **515**, 525

This paper was built using the Open Journal of Astrophysics \LaTeX template. The OJA is a journal which provides fast and easy peer review for new papers in the astro-ph section of the

arXiv, making the reviewing process simpler for authors and referees alike. Learn more at <http://astro.theoj.org>.